

M³Net: Multi-view Encoding, Matching, and Fusion for Few-shot Fine-grained Action Recognition

Hao Tang
Nanjing University of Science and
Technology
Nanjing, China
tanghao0918@njust.edu.cn

Jun Liu
Singapore University of Technology
and Design
Singapore
jun_liu@sutd.edu.sg

Shuanglin Yan
Nanjing University of Science and
Technology
Nanjing, China
shuanglinyan@njust.edu.cn

Rui Yan
Nanjing University
Nanjing, China
ruiyan@njust.edu.cn

Zechao Li
Nanjing University of Science and
Technology
Nanjing, China
zechao.li@njust.edu.cn

Jinhui Tang*
Nanjing University of Science and
Technology
Nanjing, China
jinhuitang@njust.edu.cn

ABSTRACT

Due to the scarcity of manually annotated data required for fine-grained video understanding, few-shot fine-grained (FS-FG) action recognition has gained significant attention, with the aim of classifying novel fine-grained action categories with only a few labeled instances. Despite the progress made in FS coarse-grained action recognition, current approaches encounter two challenges when dealing with the fine-grained action categories: the inability to capture subtle action details and the insufficiency of learning from limited data that exhibit high intra-class variance and inter-class similarity. To address these limitations, we propose M³Net, a matching-based framework for FS-FG action recognition, which incorporates *multi-view encoding*, *multi-view matching*, and *multi-view fusion* to facilitate embedding encoding, similarity matching, and decision making across multiple viewpoints. *Multi-view encoding* captures rich contextual details from the intra-frame, intra-video, and intra-episode perspectives, generating customized higher-order embeddings for fine-grained data. *Multi-view matching* integrates various matching functions enabling flexible relation modeling within limited samples to handle multi-scale spatio-temporal variations by leveraging the instance-specific, category-specific, and task-specific perspectives. *Multi-view fusion* consists of matching-predictions fusion and matching-losses fusion over the above views, where the former promotes mutual complementarity and the latter enhances embedding generalizability by employing multi-task collaborative learning. Explainable visualizations and experimental results on three challenging benchmarks demonstrate the superiority of M³Net in capturing fine-grained action details and achieving state-of-the-art performance for FS-FG action recognition.

CCS CONCEPTS

• **Computing methodologies** → **Activity recognition and understanding.**

KEYWORDS

fine-grained recognition, few-shot learning, action recognition

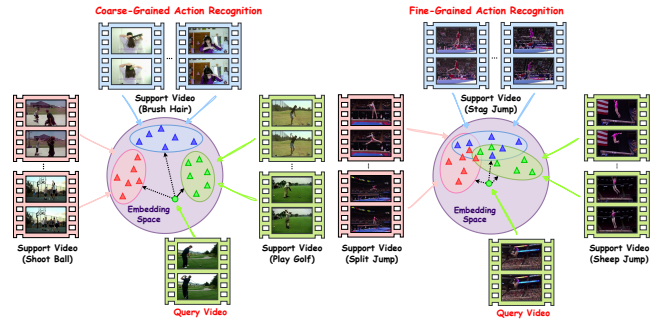


Figure 1: Coarse vs. fine-grained action recognition in the 3-way 2-shot setting. Left: Coarse-grained action recognition requires differentiating visual appearance cues of objects and backgrounds extracted from limited frames. Right: Fine-grained action recognition requires robust temporal reasoning at varying temporal scales and effective attention to fine details within limited frames due to subtle inter-class differences in the pose, specific sequence, and duration.

1 INTRODUCTION

Action recognition has achieved remarkable progress in video understanding, which is significantly driven by the introduction of large-scale datasets [5, 11, 30] and video models [7, 49, 59]. However, the current approaches heavily depend on sufficient manually annotated samples [40, 47], which require significant labor and time resources to obtain, especially for fine-grained action categories. This bottleneck hinders further progress in video understanding. Thus, few-shot (FS) action recognition [9, 10, 63] has attracted significant attention in addressing these constraints by reducing the need for manual annotations. The objective is to classify an unseen query video by assigning it to one of the action categories within the support set, even with limited annotated samples per action category. In this paper, we investigate the few-shot action recognition task in a more challenging setting, *i.e.*, few-shot fine-grained (FS-FG) action recognition, where only a few or even one labeled sample is available to recognize novel fine-grained actions.

Recent efforts have yielded great success in FS image classification [25, 42, 43, 57], thereby prompting attempts to extend this

*Corresponding author.

paradigm to the domain of action recognition for FS video classification [14, 19, 62, 65]. These methods focus on coarse-grained action categories with different visual appearances, e.g., “Shoot Ball” vs. “Brush Hair” in Fig. 1. Discriminating between these categories can be achieved via only background context, which can play a crucial role, sometimes even more significant than the action itself [17, 18, 22]. Nevertheless, the need for action recognition at finer granularities is increasingly apparent in real-world scenarios such as sports analytics [53–55] and video surveillance [33–35, 52], which usually requires a detailed comparison between similar actions with only subtle inter-class differences, e.g., “Split Jump” vs. “Sheep Jump” in Fig. 1. Notably, the presented fine-grained action examples from FineGym [32] involving rapid body movements and drastic deformation, where the subtle differences only occur in the poses of certain sub-action rather than the visual appearances of surrounding objects and backgrounds relied upon by coarse-grained action recognition. Hence, compared to coarse-grained recognition, recognizing fine-grained actions is significantly more challenging because of the subtle and discriminative multiple-dimension variations that existing coarse-grained methods typically fail to detect. Critically, applying existing FS action recognition methods directly to solve the FS-FG action recognition problem is not suitable.

To address the challenges presented by both *few-shot learning* and *fine-grained recognition* in the FS-FG action recognition, we delve into this specific task from three distinct aspects: 1) **Discriminative Embedding**. Given the large intra-class variance and subtle inter-class difference, capturing subtle spatial semantics and complicated temporal dynamics while minimizing unnecessary visual cues [56] is critical for successful FS-FG action recognition. We argue that this requires encoding rich contextual details to generate different customized embeddings from multiple views for a fine-grained action. 2) **Robust Matching**. Fine-grained actions involving various subactions with different speeds, orders, and offsets present difficulties in characterizing intricate spatio-temporal relations between a query video and limited support actions. Ideally, a more robust matching function should be employed from multiple dimensions to address the misalignment problem that arises from multi-scale spatio-temporal variations, as single-view temporal alignment metrics in existing methods may not suffice. 3) **Good Generalization**. To achieve optimal performance in few-shot learning, desirable models must transfer visual knowledge from the seen categories to the unseen categories, thereby tailoring task-specific discriminative representations [6] for target actions, particularly those with high intra-class variance and inter-class similarity. As such, good generalization is a critical concern for the FS-FG action recognition task.

Motivated by the aforementioned observations, we propose M^3 Net, a matching-based framework for FS-FG action recognition. M^3 Net consists of **multi-view encoding**, **multi-view matching**, and **multi-view fusion**, which jointly facilitates embedding learning, similarity matching, and decision making across multiple views. In the *multi-view encoding*, we argue that the relevant relationships within a frame, a video, and an episode are desirable to generate customized features that are discriminative for intra-class and inter-class variance. Initially, an *intra-frame context encoding* (IFCE) module captures subtle spatial semantics within a frame, allowing for the learning of instance-specific embeddings for fine-grained

actions. Subsequently, an *intra-video context encoding* (IVCE) module captures complex temporal dynamics within a video, enabling learning of category-specific embeddings for fine-grained actions. Meanwhile, an *intra-episode context encoding* (IECE) module infers discriminative interactive clues within an episode, facilitating learning of task-specific embeddings for few-shot tasks. The enriched higher-order embeddings from multiple views are then utilized in the *multi-view matching*, which enables flexible relation modeling and robust video matching in the limited samples. This is achieved using three proposed spatio-temporal matching functions: *instance-specific*, *category-specific*, and *task-specific* matching. Finally, we decouple *multi-view fusion* of M^3 Net into *matching-losses fusion* and *matching-predictions fusion* to guide the model to learn generalized embeddings and make a robust decision via a multi-task collaborative learning paradigm. We evaluate M^3 Net on three challenging fine-grained action recognition benchmarks (i.e., Diving48 [20], Gym99 [32], and Gym288 [32]) and achieve remarkable performance improvements over current state-of-the-art methods.

Our contributions can be summarized as follows: (1) We propose a matching-based few-shot learning framework called M^3 Net for fine-grained action recognition, which employs a multi-task collaborative learning paradigm combining *multi-view encoding*, *multi-view matching*, and *multi-view fusion*. (2) To generate customized representations with discriminative spatio-temporal cues, we propose a *multi-view encoding* procedure that captures rich contextual details from the view of intra-frame, intra-video, and intra-episode. (3) To address multi-scale spatio-temporal variations in fine-grained videos, we introduce three novel matching functions that model higher-order relations among limited samples in a *multi-view matching* process. (4) We instantiate the proposed *multi-view fusion* in M^3 Net as *matching-losses fusion* and *matching-predictions fusion* to foster cooperation and complementarity among multiple views.

2 RELATED WORK

2.1 Few-shot Learning

Inspired by the data-efficient cognitive abilities of humans, the few-shot learning (FSL) task aims to learn new concept representations with limited supervised information [51]. Recent research has investigated the FSL problem in various domains, including image classification [21, 25], object detection [1, 16], and segmentation [36, 39, 58]. Existing FSL methods commonly follow a promising meta-learning paradigm, seeking to extract task-level knowledge across different episodes [8] and generalize the learned meta-knowledge to previously unseen tasks. General FSL methods can be roughly divided into three main categories based on the type of meta-knowledge acquired: optimization-based, metric-based, and augmentation-based methods. Optimization-based approaches [8, 15, 38] aim to learn optimal initialization parameters that enable quick adaptation to novel tasks with limited update steps. Augmentation-based approaches [12, 31, 42] seek to increase the number of training samples or improve the diversity of feature distributions to augment model training. Metric-based approaches [37, 41, 45, 46] aim to learn an embedding space and compare the similarity between query and support images using different distance metrics. Our work is inspired by the metric-based ProtoNet [37], which builds robust category prototypes for each

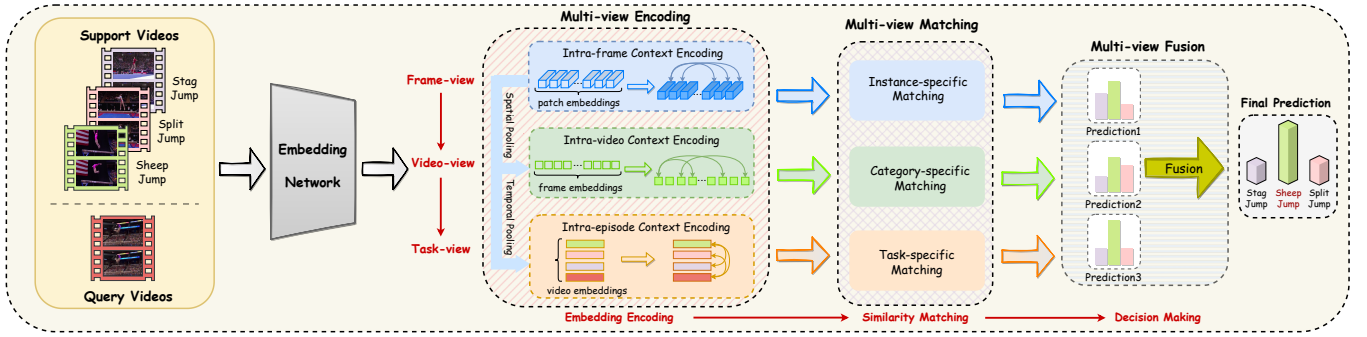


Figure 2: Schematic illustration of the proposed M³Net. Initially, given an episode of fine-grained videos, an embedding network is employed to extract their feature vectors. Subsequently, the *multi-view encoding* is utilized to capture contextual details and generate customized higher-order embeddings. The resulting embeddings are then employed in the *multi-view matching* to provide flexible relation modeling and robust video matching. Finally, the matching predictions from multiple views are merged in the *multi-view fusion* to make a robust decision.

category and makes label predictions using nearest neighbor search. We share the same insight in a more challenging FS-FG action recognition task but focus on spatial-to-temporal relations modeling and matching across multiple views.

2.2 Few-shot Action Recognition

Few-shot (FS) action recognition aims at learning to classify an unseen query action into one of the support action categories with extremely limited annotated samples [27–29], which has attracted much attention recently. However, it differs from the previous FSL approaches, which are designed for two-dimensional images. This is because the task of FS action recognition takes place in a higher-dimensional space that incorporates temporal information from video frames. The earliest research of FS action recognition could be traced back to CMN [63], which proposed a compound memory network employing a multi-saliency embedding algorithm to improve video representations for matching. Today, research in this field primarily concentrates on the metric-based meta-learning paradigm that can be categorized into two main directions: *aggregation-based* and *matching-based* methods. The former group [2, 3, 60, 63] concerns itself with the semantic modeling of context to produce video-level representations that are used for determining similarities. The latter group [4, 26, 50, 61] focuses on explicit or implicit temporal context modeling for aligning frame-level sequences for the ultimate video matching. However, these methods concentrate solely on frame-wise matching, resulting in a lack of focus on higher-level temporal relations among multiple frames. Thus, some methods [26, 44] propose to align tuples of different sub-sequences utilizing enriched higher-order temporal representations to establish query-specific video matching. In addition to standard RGB frames, some works also utilize additional input to explicitly capture temporal clues, such as depth data [10] and compressed domain data [23]. Notably, unlike previous FS action recognition methods that focus primarily on coarse-grained action categories, this study is concerned with *fine-grained* action categories. As a result, it is less optimal to apply them directly to FS-FG action recognition, as the scarcity of fine-grained data may result in overfitting. In this paper, we propose a departure from the established paradigm by exploiting the *structural invariance* of multiple views for fine-grained

actions. This allows FS-FG action recognition to be approached as a multi-task collaborative learning task with spatial-to-temporal context modeling, receiving added advantages from the mutual complementary of multi-view matching functions.

3 METHOD

3.1 Problem Formulation

Following the conventional FS image recognition setup [21, 42, 43], the fine-grained action recognition dataset is separated into a base set $D_{\text{base}} = \{(x_i, y_i) | y_i \in C_{\text{base}}\}$ and a novel set $D_{\text{novel}} = \{(x_i, y_i) | y_i \in C_{\text{novel}}\}$, wherein y_i represents the action label of video x_i and the base and novel action categories are disjoint, *i.e.*, $C_{\text{base}} \cap C_{\text{novel}} = \emptyset$. The goal of FS-FG action recognition involves training a model or optimizer on D_{base} , which contains abundant training samples per base category, and subsequently, generalizing its performance to classify an *unseen* query action in D_{novel} using only a few annotated support samples/shots. Formally, in the N -way K -shot setting, a few-shot task (*i.e.*, *episode*) sampled from D_{novel} comprises of a support set \mathcal{S} and a query set \mathcal{Q} . The support set consists of N different action categories, *i.e.*, $C_{\text{support}} \subseteq C_{\text{novel}}$. Each category comprises K support video clips, where K typically ranges from 1 to 5. Thus, the objective is to recognize a query video $V_j \in \mathcal{Q}$ as one of the support action categories with the aid of support samples $\mathcal{S} = \{V_1, \dots, V_{N \times K}\}$. Consistent with previous methods [4, 44, 50], we adopt an episodic training paradigm [46] to sample numerous training episodes, which guarantees faithful training in the test environment.

3.2 Overall Framework

As illustrated in Fig. 2, we propose M³Net, a matching-based few-shot learning framework that enables fine-grained recognition through a multi-task collaborative learning paradigm. Our design is to achieve complementary embedding learning, similarity matching, and metric-decision making in a three-step process: *multi-view encoding*, *multi-view matching*, and *multi-view fusion*.

Multi-view encoding: To address intra-class and inter-class variance in fine-grained actions, we introduce the *intra-frame context encoding* (IFCE) module as a spatial pathway to supplement

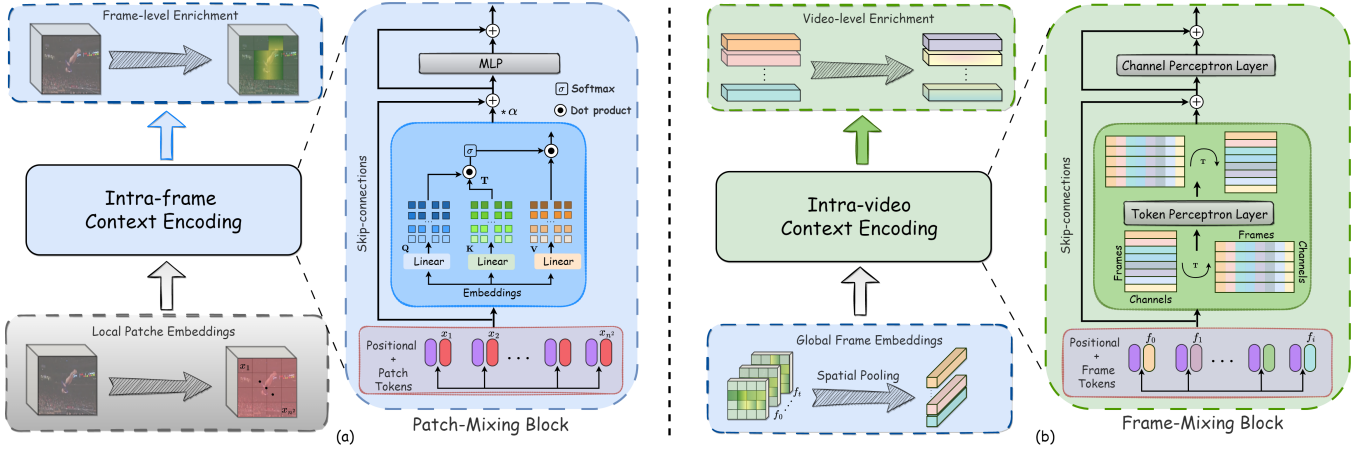


Figure 3: Illustration of the proposed Intra-frame Context Encoding module and Intra-video Context Encoding module.

instance-specific semantic information using patch-level spatial context within a frame. Additionally, we introduce the *intra-video context encoding* (IVCE) module as a temporal pathway to dynamically capture motion-specific temporal context within a video. Our approach also includes the *intra-episode context encoding* (IECE) module, serving as a task-adaptive pathway to capture discriminative task-specific cues across videos in an episode, mitigating inter-class variance of fine-grained actions.

Multi-view matching: Three novel spatio-temporal matching functions are suggested in M^3 Net, namely *instance-specific*, *category-specific*, and *task-specific* matching, based on video embeddings enhanced by the IFCE, IVCE, and IECE modules. To handle multi-scale spatio-temporal variations in fine-grained actions, we first propose the *instance-specific* matching function for frame-level enriched features. For video-level enriched features and task-level enriched features, the proposed *category-specific* and *task-specific* matching functions make full use of limited available samples to facilitate flexible and robust video matching.

Multi-view fusion: To encourage generalized embeddings and improve decision-making abilities in a multi-task learning framework, we integrate diverse losses and predictions of multiple matching branches presented in the previous multi-view matching process. Empirically, the proposed *multi-view fusion* procedure amplifies matching diversity and enhances the embedding generalization, ultimately benefitting FS-FG action recognition.

3.3 Multi-view Encoding

3.3.1 Intra-frame Context Encoding. The IFCE module aims to emphasize instance-specific semantics by utilizing spatial-based patch interaction within each frame of a fine-grained video. In essence, the IFCE module effectively manages the impact of class-irrelevant visual cues during feature transformation, consequently permitting subsequent *instance-specific* matching.

Formally, let $f_i \in \mathbb{R}^{h \times w \times d}$ denotes the feature map of i -th frame in a video, comprising $h \times w$ patches with a d -dimensional embedding. Instead of using the entire spatial position [48], an adaptive pooling operation is employed to transform f_i into $n \times n$ ($n \ll h/w$)

non-overlapping local patches (also referred to as *tokens*), which effectively limits the computation consumed by dot-product operation across the spatial dimension. As shown in Fig. 3(a), the core of the IFCE module is a *patch-mixing block* that explicitly captures rich contextual information across all patches, with the sequence of patches $Z_i = ([f_i^1, f_i^2, \dots, f_i^{n \times n}] + P) \in \mathbb{R}^{n^2 \times d}$ passed through it, where a learned positional embedding $P \in \mathbb{R}^{n^2 \times d}$ is added to the patches to retain positional information. To learn discriminative contextual information, the input Z_i is transformed into (Z_i^q, Z_i^k, Z_i^v) triplets using three matrices $W_Q, W_K, W_V \in \mathbb{R}^{d \times d}$ as $Z_i^q = Z_i W_Q$, $Z_i^k = Z_i W_K$, and $Z_i^v = Z_i W_V$. Given that Z_i^q , Z_i^k and Z_i^v share the same input source, patch-level interaction can be described as:

$$\hat{Z}_i = \alpha \cdot \text{Softmax} \left(\frac{Z_i^q \cdot Z_i^k \top}{\sqrt{d}} \right) \cdot Z_i^v + Z_i, \quad (1)$$

where $\text{Softmax}(\cdot)$ is a row-wise softmax function used to determine the interaction weight between the patches, and α is an adaptive learning weight initialized to 1 for residual learning. The pairwise similarity between patches in Z_i^q and Z_i^k defines the attention scores computed by the dot-product operation and is further used to produce the final weighted output Z_i^v . The patch-attended feature \hat{Z}_i is passed through an MLP block to generate the final spatial context-aware feature as $f'_i = \text{MLP}(\hat{Z}_i) + \hat{Z}_i$ where the MLP comprises three linear projections separated by two ReLU non-linearity.

3.3.2 Intra-video Context Encoding. The previously discussed IFCE module aims to effectively discover subtle spatial semantics in the individual video frames. However, it encounters challenges when considering complex fine-grained actions that involve different orders and offsets. Because the IFCE module relies solely on the spatial perspective rather than considering multi-scale temporal variations from a temporal perspective. To address this limitation, we introduce an additional *intra-video context encoding* (IVCE) module that functions as a temporal pathway, which is capable of adaptively capturing long-range temporal dynamics within a video and augmenting all frame features with their temporal context.

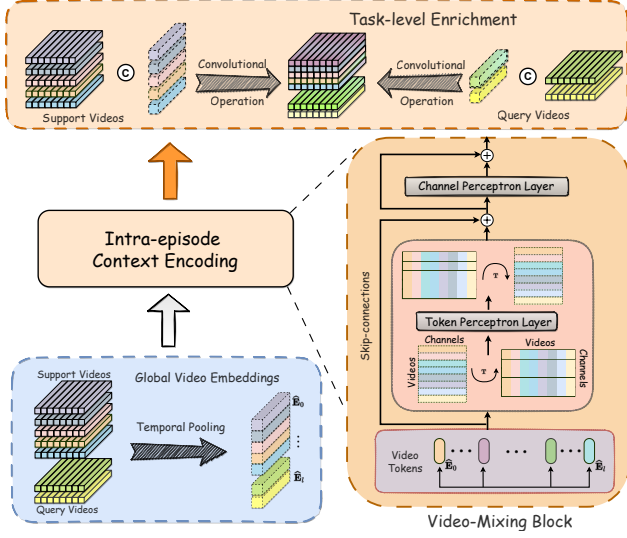


Figure 4: Illustration of the proposed Intra-episode Context Encoding module.

Formally, let the input video sequence $\mathbf{v}_j \in \mathbb{R}^{t \times n^2 \times d}$ be enriched by the IFCE module for the j -th video containing t frames in an episode. We apply an average pooling operation to squeeze the spatial dimension of \mathbf{v}_j to generate the frame-level global representations, denoted as $\mathbf{V}_j \in \mathbb{R}^{t \times d}$, and introduce a learned positional embedding $\mathbf{P} \in \mathbb{R}^{t \times d}$ applied to \mathbf{V}_j to encode temporal order information among frames. As illustrated in Fig. 3(b), the core of the IVCE module is a *frame-mixing block*, and all tokens are concatenated as input of this block to update the frame-level feature. Specifically, a *token perception layer*, which first applies to a transposed input table \mathbf{V}_j^T for frame-mixing refinement, is shared across the token dimension d and followed by a *channel perception layer* for channel-mixing refinement, which is shared across the frame tokens t . Both layers consist of two fully-connected layers separated by a ReLU non-linearity. The whole process can be written as follows:

$$\begin{aligned} \hat{\mathbf{V}}_j &= \text{ReLU}(\mathbf{V}_j^T \mathbf{W}_{t_1}) \mathbf{W}_{t_2} + \mathbf{V}_j^T, \\ \mathbf{V}'_j &= \text{ReLU}(\hat{\mathbf{V}}_j^T \mathbf{W}_{c_1}) \mathbf{W}_{c_2} + \hat{\mathbf{V}}_j^T, \end{aligned} \quad (2)$$

where $\mathbf{W}_{t_1}, \mathbf{W}_{t_2} \in \mathbb{R}^{t \times t}$ and $\mathbf{W}_{c_1}, \mathbf{W}_{c_2} \in \mathbb{R}^{d \times d}$ are four learnable weights. The output enriched video sequence feature is denoted as $\mathbf{V}'_j \in \mathbb{R}^{t \times d}$, which is obtained by reshaping the temporally-enriched features back to the original token's dimensions. The designed *token perception layer* and *channel perception layer* allow interaction of different tokens and communication between different channels to refine each frame with temporal relational context.

3.3.3 Intra-episode Context Encoding. The IFCE and IVCE modules enhance the original video representation in both spatial and temporal dimensions, highlighting class-specific representations and reducing intra-class variance. However, due to the small inter-class variance of fine-grained actions, the above task-agnostic embeddings are susceptible to overfitting the cues of the seen categories, which may impede good generalization in FS-FG action

recognition. To mitigate this, we introduce the IECE module as a task-adaption pathway that captures discriminative interactive clues across videos. This allows for co-adaptation between videos in an episode to obtain task-specific embeddings.

Fig. 4 illustrates the core of the IECE module, namely *video-mixing block*. This shares the same architecture as the *frame-mixing block* in the IVCE module but differs in its usage and purpose. Given an input episode (*i.e.*, a few-shot task) \mathbf{e} containing the features of l video clips, in which t frames in each video are enriched ahead by the IFCE module, we first squeeze the spatial dimension of all features in \mathbf{e} to obtain the global frame-level embeddings $\mathbf{E} \in \mathbb{R}^{l \times t \times d}$. We then proceed to squeeze the temporal dimension of \mathbf{E} to acquire the global video-level embeddings $\hat{\mathbf{E}} \in \mathbb{R}^{l \times d}$ for the entire episode. Each video's global embedding $\hat{\mathbf{E}}_i \in \mathbb{R}^d$ is regarded as a token and we input all tokens to the *video-mixing block* to update the video-level feature. Since the *token perception layer* in the *video-mixing block* is insensitive to the order of the input videos, we cannot use position embedding for $\hat{\mathbf{E}}$. Detailedly, the process of the *video-mixing block* is similar to Eq. 2, wherein the *token perception layer* facilitates the interaction of all videos within an episode while considering the semantic relationships among different videos, and the *channel perception layer* semantically contextualizes the video instances with relational context. Finally, the output of the *video-mixing block* serves as meta weights that help contextualize all video-level embeddings in \mathbf{E} , to enable strong co-adaptation of each item by a learnable *convolution layer*. Therefore, the proposed IECE module achieves an implicit alignment effect on different videos, thus making all embeddings task-specific for subsequent task-specific matching.

3.4 Multi-view Matching

The proposed *multi-view encoding* in the preceding section captures intra-frame, intra-video, and intra-episode contexts to enhance the sub-sequence representations for matching. To ensure mutually complementary capabilities, customized matching functions are employed in *multi-view matching* for the enriched video representations, which involves two types of matching functions, namely *temporal* and *non-temporal*, depending on the utilization of temporal information. Specifically, *instance-specific* matching (I-M) as a *temporal* function is utilized for embeddings enriched by the IFCE module, while *category-specific* matching (C-M) and *task-specific* matching (T-M) as two *non-temporal* functions are adopted for embeddings enriched by the IVCE and IECE modules, respectively.

3.4.1 Instance-specific Matching. After enriching the embeddings with the IFCE module, we apply the proposed *instance-specific* matching function to match the query video $\mathbf{V}_j = \{\mathbf{f}_y^j\}_{y=1}^t \in \mathbb{R}^{t \times d}$ and support video $\mathbf{V}_i = \{\mathbf{f}_x^i\}_{x=1}^t \in \mathbb{R}^{t \times d}$, where t denotes the number of frames and d indicates the dimension of frame-level embedding. Since the IFCE module does not incorporate temporal information, we align the frames of the two videos and infer the ordered temporal alignment score as a video-to-video similarity. Based on inspired work from OTAM [4], we first calculate the pairwise matching matrix $\mathbf{M}_{ij} \in \mathbb{R}^{t \times t}$, where $\mathbf{M}_{ij}(x, y)$ represents the cosine distance between the x -th frame of video \mathbf{V}_j

and y -th frame of video V_j , i.e., $M_{ij}(x, y) = 1 - \frac{f_x^i \cdot f_y^j}{\|f_x^i\| \|f_y^j\|}$. Subsequently, we employ *Dynamic Time Wrapping* [24] for calculating the minimum cumulative matching costs over the units in M_{ij} via dynamic programming. Finally, we average the similarities over the optimal path with the minimum cumulative cost on M_{ij} to produce the video-to-video similarity, i.e., $D_{ij}(x, y) = M_{ij}(x, y) + \min\{D_{ij}(x-1, y-1), D_{ij}(x-1, y), D_{ij}(x, y-1)\}$, where $1 \leq x \leq t$ and $1 \leq y \leq t$. We average the pairwise video-to-video similarities between the query and all support videos, which yields the final score \mathcal{D}_1^c for class c .

3.4.2 Category-specific Matching. After acquiring embeddings enriched by the IVCE module for the support video and query video, we construct a *query-centered prototype reconstruction* through a cross-attention process from the query samples to the support prototype. Specifically, we stack all frame embeddings from each support video to obtain the class prototype V^c for each action class c . Given a query video clip $V_j \in \mathbb{R}^{t \times d}$, the reconstructed prototype is formulated as $\hat{V}^c = \text{Softmax}\left(\frac{V_j W_Q (V^c W_K)^T}{\sqrt{d_k}}\right) V^c W_V$, where $W_Q/W_K/W_V \in \mathbb{R}^{d \times d_k}$. Next, the distances between the frame embeddings of a query video and the reconstructed c -th class prototype are aggregated to obtain the distance as $D_c^{q \rightarrow s} = \|V_j W_V - \hat{V}^c\|$. However, focusing solely on the query-specific prototype is sub-optimal for making full use of limited training data. Therefore, we propose a *prototype-centered query reconstruction* by applying the same cross-attention process from the support set to the query set. Then, the distances between the reconstructed frame embeddings of the query video and the c -th class prototype are aggregated to obtain $D_c^{s \rightarrow q}$. Finally, the sum of the two distances is used for classifying the query action for class c , i.e., $\mathcal{D}_2^c = D_c^{s \rightarrow q} + D_c^{q \rightarrow s}$.

3.4.3 Task-specific Matching. Given the support video V_i and the query video V_j , let $V_i = \{f_x^i\}_{x=1}^t$, $V_j = \{f_y^j\}_{y=1}^t \in \mathbb{R}^{t \times d}$ denote the sets of clip features enriched by the IECE module. Considering that both the support and query videos are contextualized in a task-specific manner, which achieves an implicit alignment effect, each frame in the query set is matched with its closest frame in the support set, and all query frame scores are averaged to obtain the final video-to-video similarity as $D_j^i = \frac{1}{t} \sum_{f_x^i \in V_i} \left(\min_{f_y^j \in V_j} \|f_x^i - f_y^j\| \right)$. Similar to *category-specific* matching function, we derive the symmetric process in this function where every frame from the support set must match jointly as $D_i^j = \frac{1}{t} \sum_{f_y^j \in V_j} \left(\min_{f_x^i \in V_i} \|f_y^j - f_x^i\| \right)$. The similarity score between the two videos is calculated as $D_{ij} = D_j^i + D_i^j$. We average the similarity scores between the query video and all support videos in class c to obtain the final score \mathcal{D}_3^c for this class.

3.5 Multi-task Learning with Multi-view Fusion

To strengthen the collaborative power of *multi-view encoding* and amalgamate the contributions of diverse *multi-view matching* functions, we reformulate the optimization of the proposed framework as a multi-task collaborative learning paradigm and boost performance from a *multi-view fusion* perspective, as displayed in Fig. 2.

In doing so, we decouple the proposed *multi-view fusion* of M³Net into *matching-losses fusion* and *matching-predictions fusion* to facilitate the model in learning generalized embeddings and to make a robust decision to accomplish complementarity among multiple views. During training, given the ground-truth class labels $Y^q \in \mathbb{R}^N$ for N -way K -shot settings, the similarity scores $\mathcal{D}_1, \mathcal{D}_2, \mathcal{D}_3$ from Sec. 3.4 are passed through *softmax* to obtain class probabilities $Y_1, Y_2, Y_3 \in \mathbb{R}^N$, which are individually optimized via cross-entropy loss. Thus, the classification loss for each matching branch can be formulated as $\mathcal{L}_1 = \text{CE}(Y_1, Y^q)$, $\mathcal{L}_2 = \text{CE}(Y_2, Y^q)$, and $\mathcal{L}_3 = \text{CE}(Y_3, Y^q)$, where $\text{CE}(\cdot)$ refers to the cross-entropy loss function. As a result, the comprehensive *matching-losses fusion* is delineated as $\mathcal{L} = \mathcal{L}_1 + \mathcal{L}_2 + \mathcal{L}_3$ for learning generalized spatial-temporal embeddings. At the inference stage, we construct a comprehensive multi-view predictor by summing the prediction distribution of individual matching branches as follows: $Y = Y_1 + Y_2 + Y_3$.

4 EXPERIMENTS

4.1 Datasets

We evaluate the effectiveness of our proposed M³Net against other competing methods on two common fine-grained action recognition datasets, namely FineGym [32] and Diving48 [20], using 5-way 1/3/5-shot FS recognition tasks for all models considered. To ensure the reliability of the results, we devise carefully-planned evaluation protocols for both datasets. Specifically, we determine the split of training, validation, and testing action categories, as well as the number of samples in each episode.

FineGym provides annotations of hierarchical fine-grained actions in gymnastic events, which comprise two levels of fine-grained categories, namely **Gym99** and **Gym288**, with over 34k (99 classes) and 38k (288 classes) samples respectively. In the case of **Gym99**, a 61/12/26 split is employed for the training/validation/testing categories. Due to insufficient support samples for multi-shot tasks, some actions in **Gym288** are excluded, which results in the splits of training/validation/testing categories being set to 128/25/61.

Diving48 is a fine-grained video dataset of competitive diving, consisting of 18,404 trimmed video clips of 48 well-defined dive sequences. This proves to be a challenging task for fine-grained action recognition as dives may differ in different stages and thus require modeling of long-term temporal dynamics. Here, we randomly select 28 training, 5 validation, and 15 testing categories.

4.2 Implementation Details

Following the previous works [4, 44, 50], we employ ResNet-50 [13] as the embedding model and initialize it with weights pre-trained on the ImageNet dataset [30]. To accurately represent each fine-grained action, we uniformly and sparsely sample 8 frames per video (i.e., $t = 8$) as in previous methods [44, 50]. We employ an IFCE module by setting $n = 4$, where f_i has a dimension of $d = 2048$. During the training phase, the input video frames are randomly cropped to 224×224 , we introduce basic data augmentation techniques including random cropping and random horizontal flip. The optimizer used to optimize our M³Net is the SGD optimizer having an initialized learning rate of $1e - 4$. The training procedure continues for 60,000 episodes on all datasets with the learning rate decaying by 0.5 after every 2,000 episodes. During the inference

Table 1: Comparison of 1-shot, 3-shot, and 5-shot recognition performance on the Diving48, Gym99 and Gym288 datasets.

Method	Reference	Diving48			Gym99			Gym288		
		1-shot	3-shot	5-shot	1-shot	3-shot	5-shot	1-shot	3-shot	5-shot
TSN[49]+Cosine	ECCV'16	29.72 ± 0.25	35.69 ± 0.26	38.81 ± 0.26	36.63 ± 0.30	41.35 ± 0.31	42.76 ± 0.31	36.68 ± 0.29	42.87 ± 0.29	44.82 ± 0.30
ProtoNet [37]	NeurIPS'17	59.80 ± 0.33	74.74 ± 0.29	77.69 ± 0.28	62.99 ± 0.36	74.25 ± 0.31	77.99 ± 0.30	58.98 ± 0.35	70.56 ± 0.31	74.87 ± 0.30
OTAM [4]	CVPR'20	41.64 ± 0.29	47.96 ± 0.27	49.78 ± 0.26	48.93 ± 0.35	52.88 ± 0.32	55.61 ± 0.32	47.58 ± 0.33	53.67 ± 0.31	55.62 ± 0.31
PAL [64]	BMVC'21	50.40 ± 0.24	57.57 ± 0.27	61.17 ± 0.27	58.85 ± 0.31	65.13 ± 0.32	68.64 ± 0.33	58.32 ± 0.32	63.62 ± 0.34	65.77 ± 0.35
TRX [26]	CVPR'21	62.53 ± 0.32	77.81 ± 0.29	82.01 ± 0.26	66.55 ± 0.33	80.15 ± 0.30	83.86 ± 0.27	64.03 ± 0.35	76.73 ± 0.30	81.05 ± 0.27
STRM [44]	CVPR'22	62.29 ± 0.34	77.79 ± 0.29	81.03 ± 0.27	68.09 ± 0.34	80.93 ± 0.29	84.33 ± 0.26	64.81 ± 0.36	76.98 ± 0.31	80.64 ± 0.28
HyRSM [50]	CVPR'22	61.04 ± 0.30	76.04 ± 0.30	81.74 ± 0.28	67.09 ± 0.33	78.15 ± 0.32	82.92 ± 0.31	62.86 ± 0.35	73.12 ± 0.32	78.81 ± 0.31
M ³ Net	Ours	72.35 ± 0.33	82.50 ± 0.26	85.44 ± 0.24	72.70 ± 0.33	83.03 ± 0.27	86.71 ± 0.24	68.66 ± 0.34	79.73 ± 0.29	83.05 ± 0.26

Table 2: Impact of the key components in multi-view encoding on Gym99 for 5-way 1-shot action recognition. To simplify, the intra-frame, intra-video, and intra-episode context encoding are represented as "I-F", "I-V", and "I-E", respectively.

Fusion Num		1	1	1	1	1	1	1	
Multi-view Encoding	I-F	-	✓	-	-	✓	-	✓	
	I-V	-	-	-	✓	✓	-	✓	
	I-E	-	-	-	-	-	✓	✓	
Multi-view Matching	I-M	✓	✓	-	-	-	-	-	
	C-M	-	-	✓	✓	✓	-	-	
	T-M	-	-	-	-	-	✓	✓	
Fusion	Y	46.53	50.09	64.66	68.92	69.53	44.50	58.15	59.79

phase, we resize all inputs to 256×256 before center cropping. We perform 5-way 1/3/5-shot evaluation for FS-FG action recognition on all datasets and report the mean accuracy obtained from 6,000 episodes randomly selected from the testing set.

4.3 Comparison with state-of-the-art

This section presents a comparative evaluation of state-of-the-art FS action recognition methods for the standard 5-way 1/3/5-shot task on three fine-grained benchmarks, considering only methods employing a 2D embedding backbone (*i.e.*, ResNet50) for per-frame features extraction. Our proposed M³Net significantly outperforms existing methods, setting a new state-of-the-art on all three benchmarks, as demonstrated in Tab. 1. On Diving48, TRX [26], STRM [44], and HyRSM [50] achieve comparable recognition accuracies. In comparison, M³Net outperforms existing methods with a higher performance of 72.35/82.50/85.44% for 1/3/5-shot. Notably, M³Net achieves a significant performance improvement of up to 18.52% in the most challenging 1-shot setting. Moreover, the dataset Diving48 involves appearance-related scene understanding, while the Gym99 and Gym288 datasets primarily focus on motion-based temporal reasoning. M³Net demonstrates outstanding performance on Gym99 and Gym288 under the 1/3/5-shot settings, showcasing its ability to learn discriminative fine-grained differences from limited and similar samples. Overall, M³Net is more comprehensive in reflecting actual distances between videos and demonstrates strong robustness and generalization across these fine-grained datasets with superior performance on few-shot tasks.

Observations from the results in Tab. 1 indicate that: (1) Coarse-grained action recognition models are unsuitable for fine-grained tasks, as M³Net consistently outperforms the most advanced temporal alignment method [44] and hybrid relation method [50] for

Table 3: Comparison between different combinations of multi-view matching functions for 5-way 1/5-shot action recognition on Gym99.

Intra-frame Context Encoding	I-M	✓	-	-	✓	✓
	C-M	-	✓	-	-	-
	T-M	-	-	✓	-	-
Intra-video Context Encoding	I-M	✓	-	-	-	-
	C-M	-	✓	-	-	✓
	T-M	-	-	✓	✓	-
Intra-episode Context Encoding	I-M	✓	-	-	-	-
	C-M	-	✓	-	✓	-
	T-M	-	-	✓	-	✓
Fusion (1-shot)	Y	68.05	72.05	68.13	72.22	72.70
Fusion (5-shot)	Y	73.08	85.40	75.37	82.64	86.71

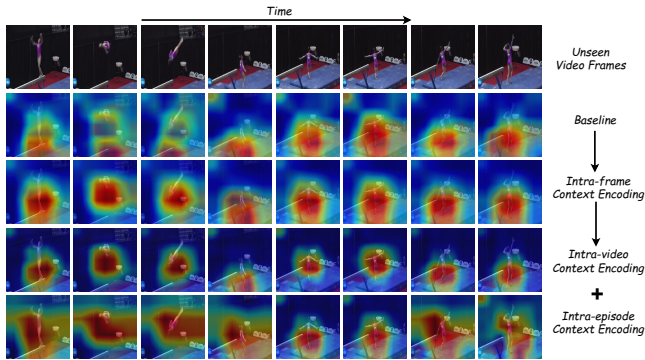
all shot settings. (2) Although STRM [44] utilizing enriched tuples outperforms other methods, it does not work well on FS-FG action recognition tasks as it utilizes sparsely sampled frame tuples as input without considering task-specific features, resulting in missing fine-grained action details. (3) HyRSM [50] shares similar insights with M³Net to generate task-specific features. However, its performance is slightly behind TRX [26] and STRM [44], as the learned task-specific feature in HyRSM is not discriminative for fine-grained actions and the single matching function is susceptible to noise interference.

4.4 Ablation Study

Effectiveness of multi-view encoding. Tab. 2 demonstrates the effect of various *multi-view encoding* components, alongside evaluations conducted on Gym99 using a 5-way 1-shot setup without *multi-view fusion*. Our observations reveal that individual components of *multi-view encoding* play a vital role in view-specific matching, displaying distinguishable characteristics under different combinations. Notably, intra-frame context encoding, denoted by I-F, improves instance-specific matching (*i.e.*, I-M) by 7.65%, intra-video context encoding, denoted by I-V, improves category-specific matching (*i.e.*, C-M) by 6.59%, and intra-episode context encoding, denoted by I-E, improves task-specific matching (*i.e.*, T-M) by 30.67%. Furthermore, the inputs of I-V and I-E are first augmented by I-F to enhance feature discriminability in M³Net, as displayed in Fig. 2. The proposed I-F further improves "I-V+C-M" and "I-E+T-M" by 0.88% and 2.82%, respectively, indicating the significance of enriching spatial context within each frame before modeling the temporal and task relationships.

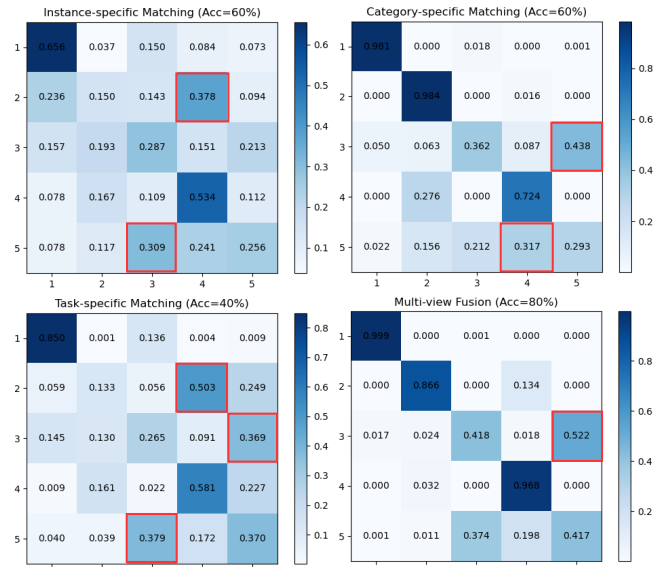
Table 4: Comparison between various combinations in multi-view fusion for 5-way 1-shot action recognition on Gym99.

Model Index		1	2	3	4	5	6	7
Fusion Num		1	1	1	2	2	2	3
Multi-view Loss	\mathcal{L}_1	✓	-	-	-	✓	✓	✓
	\mathcal{L}_2	-	✓	-	-	✓	-	✓
	\mathcal{L}_3	-	-	✓	✓	✓	-	✓
Multi-view Prediction	Y_1	50.09	-	-	-	57.93	65.59	69.35
	Y_2	-	69.53	-	70.21	-	70.60	71.82
	Y_3	-	-	59.79	68.51	59.76	-	69.89
Fusion	Y	50.09	69.53	59.79	71.81	60.94	71.47	72.70

**Figure 5: The comparison of activation map visualizations for one unseen example from the Gym99 test set.**

Influence of multi-view matching. Our proposed *multi-view matching* aims to precisely identify the most informative frame correspondences that highlight the similarity between the video pairs. We perform a comprehensive analysis of different *multi-view matching* variants by varying their constituent components, as outlined in Tab. 3. We observe that the different combinations have distinct properties, *e.g.*, **C-M** is more effective for temporal matching than **I-M** and **T-M**, thanks to the cross-attention mechanisms that operate over the query and support features. When the enriched embeddings are sufficiently discriminative, the performance of **I-M** and **T-M** is similar. However, we observe a slight degradation in the overall performance in the last column of Tab. 3 when we swap the positions of **C-M** and **T-M**, even though both matching functions are *non-temporal*, indicating the efficacy of the tailor-made matching designs for different higher-order embeddings obtained from the *multi-view* encoding.

Analysis of multi-view fusion. Further experiments are conducted on various combinations of *multi-view fusion*, and the obtained results, presented in Tab. 4, revealed the following: (i) The performance of *multi-view fusion* improves as the matching view diversity increases. (ii) Incorporating multiple matching functions through *multi-view fusion* provides superior performance compared to individual views, thus attaining a more comprehensive decision maker. As illustrated in the last column of Tab. 4, Model-7 with multi-view prediction fusion record 72.70% for **Y**, surpassing the corresponding three single-view predictions (*i.e.*, 69.35% for Y_1 , 71.82% for Y_2 , and 69.89% for Y_3 respectively). (iii) The single-view prediction (*i.e.*, Y_1 , Y_2 , and Y_3) of the full model with multi-view loss

**Figure 6: The prediction distribution shows how query videos (columns) match to support videos (rows) in robust multi-view fusion. The red box indicates the incorrect match.**

fusion surpasses that of the independent model with single-view loss, and the advantage thereof increases with the view diversity. Specifically, compared to Model-1/2/3, Model-7 exhibits an improvement in the performance of all single-view predictions from 50.09%, 69.53%, and 59.79% to 69.35%, 71.82%, and 69.89%, respectively. These results demonstrate that the proposed *multi-view fusion* guides the full model to attain more discriminative embeddings and thereby surpasses corresponding independent models.

4.5 Visualization results

Fig. 5 presents the progressive integration of our contributions in *multi-view encoding* from top to bottom, highlighting the distinctiveness of the learned context-enriched features. The integration of IFCE (third row) enhances the spatial representation of features and induces attention toward relevant objects in a single video frame. After this integration, the integration of IVCE (fourth row) further strengthens the temporal relation of features, allowing our M^3 Net to focus on the action subject while reducing attention to extraneous objects. Meanwhile, the integration of IECE (fifth row) amplifies and emphasizes task-specific regions with higher saliency, which may be more relevant for query predictions, while still retaining relatively complete original information. Additionally, Fig. 6 qualitatively shows the robustness of the proposed *multi-view fusion*. We present the prediction distribution emanating from various matching functions for a novel 5-way 1-shot task and visually demonstrate the effectiveness of the proposed *multi-view fusion*.

5 CONCLUSION

In this paper, we have proposed M^3 Net, a matching-based framework for FS-FG action recognition. The proposed framework leverages a multi-view encoding procedure, capturing rich contextual information across intra-frame, intra-video, and intra-episode views

to generate customized representations. Moreover, M³Net adopts a multi-task collaborative learning paradigm, integrating instance-specific, category-specific, and task-specific matching functions to model complex spatial and temporal relations, thereby achieving remarkable performance improvements over current state-of-the-art methods on three challenging fine-grained action recognition benchmarks. Our findings provide valuable insight for future research to exploit the *structural invariance* of multiple views to capture subtle spatial semantics and complex temporal dynamics for fine-grained video understanding, especially under the condition of data scarcity. This has broad practical implications for multimedia domains such as sports analytics and video surveillance.

REFERENCES

- [1] Simone Antonelli, Danilo Avola, Luigi Cinque, Donato Crisostomi, Gian Luca Foresti, Fabio Galasso, Marco Raoul Marini, Alessio Mecca, and Daniele Pannone. 2022. Few-Shot Object Detection: A Survey. *ACM Comput. Surv.* 54, 11s (2022), 242:1–242:37.
- [2] Mina Bishay, Georgios Zoumpourlis, and Ioannis Patras. 2019. TARN: Temporal Attentive Relation Network for Few-Shot and Zero-Shot Action Recognition. In *Proceedings of the British Machine Vision Conference (BMVC)*.
- [3] Congqi Cao, Yajuan Li, Qinyi Lv, Peng Wang, and Yanning Zhang. 2021. Few-shot action recognition with implicit temporal alignment and pair similarity optimization. *Comput. Vis. Image Underst.* 210 (2021), 103250.
- [4] Kaidi Cao, Jingwei Ji, Zhangjie Cao, Chien-Yi Chang, and Juan Carlos Niebles. 2020. Few-Shot Video Classification via Temporal Alignment. In *Proceedings of the IEEE Conference on Computer Vision and Pattern Recognition (CVPR)*.
- [5] João Carreira and Andrew Zisserman. 2017. Quo Vadis, Action Recognition? A New Model and the Kinetics Dataset. In *Proceedings of the IEEE Conference on Computer Vision and Pattern Recognition (CVPR)*.
- [6] Neng Dong, Liyan Zhang, Shuanglin Yan, Hao Tang, and Jinhui Tang. 2023. Erasing, Transforming, and Noising Defense Network for Occluded Person Re-Identification. *CoRR abs/2307.07187* (2023).
- [7] Christoph Feichtenhofer, Haoqi Fan, Jitendra Malik, and Kaiming He. 2019. Slow-Fast Networks for Video Recognition. In *Proceedings of the IEEE/CVF International Conference on Computer Vision (ICCV)*.
- [8] Chelsea Finn, Pieter Abbeel, and Sergey Levine. 2017. Model-agnostic meta-learning for fast adaptation of deep networks. In *International Conference on Machine Learning (ICML)*.
- [9] Yuqian Fu, Chengrong Wang, Yanwei Fu, Yu-Xiong Wang, Cong Bai, Xiangyang Xue, and Yu-Gang Jiang. 2019. Embodied One-Shot Video Recognition: Learning from Actions of a Virtual Embodied Agent. In *ACM International Conference on Multimedia (MM)*.
- [10] Yuqian Fu, Li Zhang, Junke Wang, Yanwei Fu, and Yu-Gang Jiang. 2020. Depth Guided Adaptive Meta-Fusion Network for Few-shot Video Recognition. In *ACM International Conference on Multimedia (MM)*.
- [11] Raghav Goyal, Samira Ebrahimi Kahou, Vincent Michalski, Joanna Materzynska, Susanne Westphal, Heuna Kim, Valentin Haenel, Ingo Fründ, Peter Yianilos, Moritz Mueller-Freitag, Florian Hoppe, Christian Thureau, Ingo Bax, and Roland Memisevic. 2017. The "Something Something" Video Database for Learning and Evaluating Visual Common Sense. In *Proceedings of the IEEE/CVF International Conference on Computer Vision (ICCV)*.
- [12] Bharath Hariharan and Ross B. Girshick. 2017. Low-shot visual recognition by shrinking and hallucinating features. In *Proceedings of the IEEE/CVF International Conference on Computer Vision (ICCV)*.
- [13] Kaiming He, Xiangyu Zhang, Shaoqing Ren, and Jian Sun. 2016. Deep residual learning for image recognition. In *Proceedings of the IEEE Conference on Computer Vision and Pattern Recognition (CVPR)*.
- [14] Yifei Huang, Lijin Yang, and Yoichi Sato. 2022. Compound Prototype Matching for Few-Shot Action Recognition. In *European Conference on Computer Vision (ECCV)*.
- [15] Muhammad Abdullah Jamal and Guo-Jun Qi. 2019. Task agnostic meta-learning for few-shot learning. In *Proceedings of the IEEE Conference on Computer Vision and Pattern Recognition (CVPR)*.
- [16] Prannay Kaul, Weidi Xie, and Andrew Zisserman. 2022. Label, Verify, Correct: A Simple Few Shot Object Detection Method. In *Proceedings of the IEEE Conference on Computer Vision and Pattern Recognition (CVPR)*.
- [17] Huafeng Li, Kaixiong Xu, Jinxing Li, and Zhengtao Yu. 2022. Dual-stream Reciprocal Disentanglement Learning for domain adaptation person re-identification. *Knowl. Based Syst.* 251 (2022), 109315.
- [18] Shuang Li, Fan Li, Jinxing Li, Huafeng Li, Bob Zhang, Dapeng Tao, and Xinbo Gao. 2023. Logical Relation Inference and Multiview Information Interaction for Domain Adaptation Person Re-Identification. *IEEE Trans. Neural Networks Learn. Syst.* (2023). <https://doi.org/10.1109/TNNLS.2023.3281504>
- [19] Shuyuan Li, Huabin Liu, Rui Qian, Yuxi Li, John See, Mengjuan Fei, Xiaoyuan Yu, and Weiyao Lin. 2022. TA2N: Two-Stage Action Alignment Network for Few-Shot Action Recognition. In *Association for the Advancement of Artificial Intelligence (AAAI)*.
- [20] Yingwei Li, Yi Li, and Nuno Vasconcelos. 2018. RESOUND: Towards Action Recognition Without Representation Bias. In *European Conference on Computer Vision (ECCV)*.
- [21] Zechao Li, Hao Tang, Zhimao Peng, Guo-Jun Qi, and Jinhui Tang. 2023. Knowledge-Guided Semantic Transfer Network for Few-Shot Image Recognition. *IEEE Trans. Neural Networks Learn. Syst.* (2023). <https://doi.org/10.1109/TNNLS.2023.3240195>
- [22] Xinyu Lin, Jinxing Li, Zeyu Ma, Huafeng Li, Shuang Li, Kaixiong Xu, Guangming Lu, and David Zhang. 2022. Learning Modal-Invariant and Temporal-Memory for Video-based Visible-Infrared Person Re-Identification. In *Proceedings of the IEEE Conference on Computer Vision and Pattern Recognition (CVPR)*.
- [23] Wenyang Luo, Yufan Liu, Bing Li, Weiming Hu, Yanan Miao, and Yangxi Li. 2022. Long-Short Term Cross-Transformer in Compressed Domain for Few-Shot Video Classification. In *Proceedings of the International Joint Conference on Artificial Intelligence (IJCAI)*.
- [24] Meinard Müller. 2007. Dynamic time warping. *Information retrieval for music and motion* (2007), 69–84.
- [25] Zhimao Peng, Zechao Li, Junge Zhang, Yan Li, Guo-Jun Qi, and Jinhui Tang. 2019. Few-Shot Image Recognition With Knowledge Transfer. In *Proceedings of the IEEE/CVF International Conference on Computer Vision (ICCV)*.
- [26] Toby Perrett, Alessandro Masullo, Tilo Burghardt, Majid Mirmehdi, and Dima Damen. 2021. Temporal-Relational CrossTransformers for Few-Shot Action Recognition. In *Proceedings of the IEEE Conference on Computer Vision and Pattern Recognition (CVPR)*.
- [27] Biao Qian, Yang Wang, Richang Hong, and Meng Wang. 2023. Adaptive Data-Free Quantization. In *Proceedings of the IEEE Conference on Computer Vision and Pattern Recognition (CVPR)*.
- [28] Biao Qian, Yang Wang, Richang Hong, and Meng Wang. 2023. Rethinking Data-Free Quantization as a Zero-Sum Game. In *Association for the Advancement of Artificial Intelligence (AAAI)*.
- [29] Biao Qian, Yang Wang, Hongzhi Yin, Richang Hong, and Meng Wang. 2022. Switchable Online Knowledge Distillation. In *European Conference on Computer Vision (ECCV)*.
- [30] Olga Russakovsky, Jia Deng, Hao Su, Jonathan Krause, Sanjeev Satheesh, Sean Ma, Zhiheng Huang, Andrej Karpathy, Aditya Khosla, Michael S. Bernstein, Alexander C. Berg, and Fei-Fei Li. 2015. Imagenet large scale visual recognition challenge. *Int. J. Comput. Vis.* 115, 3 (2015), 211–252.
- [31] Eli Schwartz, Leonid Karlinsky, Joseph Shtok, Sivan Harary, Mattias Marder, Abhishek Kumar, Rogério Schmidt Feris, Raja Giryes, and Alexander M. Bronstein. 2018. Delta-encoder: an effective sample synthesis method for few-shot object recognition. In *Advances in Neural Information Processing Systems (NeurIPS)*.
- [32] Dian Shao, Yue Zhao, Bo Dai, and Dahua Lin. 2020. FineGym: A Hierarchical Video Dataset for Fine-Grained Action Understanding. In *Proceedings of the IEEE Conference on Computer Vision and Pattern Recognition (CVPR)*.
- [33] Fei Shen, Xiaoyu Du, Liyan Zhang, Xiangbo Shu, and Jinhui Tang. 2023. Triplet Contrastive Representation Learning for Unsupervised Vehicle Re-identification. *CoRR abs/2301.09498* (2023).
- [34] Fei Shen, Yi Xie, Jianqing Zhu, Xiaobin Zhu, and Huanqiang Zeng. 2023. GiT: Graph Interactive Transformer for Vehicle Re-Identification. *IEEE Trans. Image Process.* 32 (2023), 1039–1051.
- [35] Fei Shen, Jianqing Zhu, Xiaobin Zhu, Yi Xie, and Jingchang Huang. 2022. Exploring Spatial Significance via Hybrid Pyramidal Graph Network for Vehicle Re-Identification. *IEEE Trans. Intell. Transp. Syst.* 23, 7 (2022), 8793–8804.
- [36] Guangchen Shi, Yirui Wu, Jun Liu, Shaohua Wan, Wenhui Wang, and Tong Lu. 2022. Incremental Few-Shot Semantic Segmentation via Embedding Adaptive-Update and Hyper-class Representation. In *ACM International Conference on Multimedia (MM)*.
- [37] Jake Snell, Kevin Swersky, and Richard S. Zemel. 2017. Prototypical networks for few-shot learning. In *Advances in Neural Information Processing Systems (NeurIPS)*.
- [38] Qianru Sun, Yaoyao Liu, Tat-Seng Chua, and Bernt Schiele. 2019. Meta-transfer learning for few-shot learning. In *Proceedings of the IEEE Conference on Computer Vision and Pattern Recognition (CVPR)*.
- [39] Yanpeng Sun, Qiang Chen, Xiangyu He, Jian Wang, Haocheng Feng, Junyu Han, Errui Ding, Jian Cheng, Zechao Li, and Jingdong Wang. 2022. Singular Value Fine-tuning: Few-shot Segmentation requires Few-parameters Fine-tuning. In *Advances in Neural Information Processing Systems (NeurIPS)*.
- [40] Zehua Sun, QiuHong Ke, Hossein Rahmani, Mohammed Bannamoun, Gang Wang, and Jun Liu. 2023. Human Action Recognition From Various Data Modalities: A Review. *IEEE Trans. Pattern Anal. Mach. Intell.* 45, 3 (2023), 3200–3225.
- [41] Flood Sung, Yongxin Yang, Li Zhang, Tao Xiang, Philip H. S. Torr, and Timothy M. Hospedales. 2018. Learning to compare: Relation network for few-shot learning.

- In *Proceedings of the IEEE Conference on Computer Vision and Pattern Recognition (CVPR)*.
- [42] Hao Tang, Zechao Li, Zhimao Peng, and Jinhui Tang. 2020. BlockMix: Meta Regularization and Self-Calibrated Inference for Metric-Based Meta-Learning. In *ACM International Conference on Multimedia (MM)*.
- [43] Hao Tang, Chengcheng Yuan, Zechao Li, and Jinhui Tang. 2022. Learning attention-guided pyramidal features for few-shot fine-grained recognition. *Pattern Recognit.* 130 (2022), 108792.
- [44] Anirudh Thatipelli, Sanath Narayan, Salman Khan, Rao Muhammad Anwer, Fahad Shahbaz Khan, and Bernard Ghanem. 2022. Spatio-temporal Relation Modeling for Few-shot Action Recognition. In *Proceedings of the IEEE Conference on Computer Vision and Pattern Recognition (CVPR)*.
- [45] Sheng Tian, Hao Tang, and Longquan Dai. 2021. Coupled Patch Similarity Network FOR One-Shot Fine-Grained Image Recognition. In *Proceedings of the IEEE International Conference on Image Processing (ICIP)*.
- [46] Oriol Vinyals, Charles Blundell, Tim Lillicrap, Koray Kavukcuoglu, and Daan Wierstra. 2016. Matching networks for one shot learning. In *Advances in Neural Information Processing Systems (NeurIPS)*.
- [47] Di Wang, Jinyuan Liu, Risheng Liu, and Xin Fan. 2023. An interactively reinforced paradigm for joint infrared-visible image fusion and saliency object detection. *Inf. Fusion* 98 (2023), 101828.
- [48] Di Wang, Hao Tang, Jinshan Pan, and Jinhui Tang. 2021. Learning a Tree-Structured Channel-Wise Refinement Network for Efficient Image Deraining. In *Proceedings of the IEEE International Conference on Multimedia and Expo (ICME)*.
- [49] Limin Wang, Yuanjun Xiong, Zhe Wang, Yu Qiao, Dahua Lin, Xiaoou Tang, and Luc Van Gool. 2016. Temporal Segment Networks: Towards Good Practices for Deep Action Recognition. In *European Conference on Computer Vision (ECCV)*.
- [50] Xiang Wang, Shiwei Zhang, Zhiwu Qing, Mingqian Tang, Zhengrong Zuo, Changxin Gao, Rong Jin, and Nong Sang. 2022. Hybrid Relation Guided Set Matching for Few-shot Action Recognition. In *Proceedings of the IEEE Conference on Computer Vision and Pattern Recognition (CVPR)*.
- [51] Yang Wang. 2021. Survey on Deep Multi-modal Data Analytics: Collaboration, Rivalry, and Fusion. *ACM Trans. Multim. Comput. Commun. Appl.* 17, 1s (2021), 10:1–10:25.
- [52] Yang Wang, Jinjia Peng, Huibing Wang, and Meng Wang. 2022. Progressive learning with multi-scale attention network for cross-domain vehicle re-identification. *Sci. China Inf. Sci.* 65, 6 (2022), 1–15.
- [53] Rui Yan, Lingxi Xie, Xiangbo Shu, Liyan Zhang, and Jinhui Tang. 2023. Progressive Instance-Aware Feature Learning for Compositional Action Recognition. *IEEE Trans. Pattern Anal. Mach. Intell.* 45, 8 (2023), 10317–10330.
- [54] Rui Yan, Lingxi Xie, Jinhui Tang, Xiangbo Shu, and Qi Tian. 2020. Social Adaptive Module for Weakly-Supervised Group Activity Recognition. In *European Conference on Computer Vision (ECCV)*.
- [55] Rui Yan, Lingxi Xie, Jinhui Tang, Xiangbo Shu, and Qi Tian. 2023. HiGCIN: Hierarchical Graph-Based Cross Inference Network for Group Activity Recognition. *IEEE Trans. Pattern Anal. Mach. Intell.* 45, 6 (2023), 6955–6968.
- [56] Shuanglin Yan, Hao Tang, Liyan Zhang, and Jinhui Tang. 2022. Image-Specific Information Suppression and Implicit Local Alignment for Text-based Person Search. *CoRR* abs/2208.14365 (2022).
- [57] Zican Zha, Hao Tang, Yunlian Sun, and Jinhui Tang. 2023. Boosting Few-shot Fine-grained Recognition with Background Suppression and Foreground Alignment. *IEEE Trans. Circuits Syst. Video Technol.* 33, 8 (2023), 3947–3961.
- [58] Dong Zhang, Hanwang Zhang, Jinhui Tang, Xian-Sheng Hua, and Qianru Sun. 2020. Causal Intervention for Weakly-Supervised Semantic Segmentation. In *Advances in Neural Information Processing Systems (NeurIPS)*.
- [59] David Junhao Zhang, Kunchang Li, Yali Wang, Yunpeng Chen, Shashwat Chandra, Yu Qiao, Luoqi Liu, and Mike Zheng Shou. 2022. MorphMLP: An Efficient MLP-Like Backbone for Spatial-Temporal Representation Learning. In *European Conference on Computer Vision (ECCV)*.
- [60] Hongguang Zhang, Li Zhang, Xiaojuan Qi, Hongdong Li, Philip H. S. Torr, and Piotr Koniusz. 2020. Few-Shot Action Recognition with Permutation-Invariant Attention. In *European Conference on Computer Vision (ECCV)*.
- [61] Songyang Zhang, Jiale Zhou, and Xuming He. 2021. Learning Implicit Temporal Alignment for Few-shot Video Classification. In *Proceedings of the International Joint Conference on Artificial Intelligence (IJCAI)*.
- [62] Sipeng Zheng, Shizhe Chen, and Qin Jin. 2022. Few-Shot Action Recognition with Hierarchical Matching and Contrastive Learning. In *European Conference on Computer Vision (ECCV)*.
- [63] Linchao Zhu and Yi Yang. 2018. Compound Memory Networks for Few-Shot Video Classification. In *European Conference on Computer Vision (ECCV)*.
- [64] Xiatian Zhu, Antoine Toisoul, Juan-Manuel Pérez-Rúa, Li Zhang, Brais Martínez, and Tao Xiang. 2021. Few-shot Action Recognition with Prototype-centered Attentive Learning. In *Proceedings of the British Machine Vision Conference (BMVC)*.
- [65] Zhenxi Zhu, Limin Wang, Sheng Guo, and Gangshan Wu. 2021. A Closer Look at Few-Shot Video Classification: A New Baseline and Benchmark. In *Proceedings of the British Machine Vision Conference (BMVC)*.